Molecular Dynamics Studies on Superoxide Dismutase and Its Mutants: The Structural and Functional Role of Arg 143

Lucia Banci,* Paolo Carloni, Giovanni La Penna, and Pier Luigi Orioli

Contribution from the Department of Chemistry, University of Florence, Florence, Italy.
Received February 3, 1992

Abstract: Molecular dynamics (MD) calculations have been performed on superoxide dismutase (SOD) and on its mutants on the Arg 143 residue, which has been modified to a Glu and to a Ile residue. The simulations were performed over the entire "orange" subunit, solvated by about 3300 water molecules, and on the atoms at the subunit–subunit interface. A 10-Å residue-based cut-off for the pair interactions was used. The trajectories were calculated for 63 ps, and the last 36 ps were used for structural analysis. The set of parameters used for describing the metal ions reproduces fairly well the structure of the active site. Significantly, the semicoordinated water molecule maintains its position close to the copper ion, although in the simulation no bond has been imposed between it and the copper ion, in agreement with experimental evidence. In the wild type SOD, the active site channel shows high mobility, resulting in an increase of the open section. In particular Arg 143 is highly mobile. On the contrary, the mutants show a reduced mobility at the channel, the decrease being larger when a negative group, such as a Glu, is present on position 143 with respect to a neutral group as Ile. This behavior is related to the catalytic activity of SOD and its mutants here investigated, and a role of the extent of the mobility of the residues hanging in the active site channel on the enzymatic reaction is proposed.

Introduction

Superoxide dismutase (SOD) is a dimeric enzyme which contains a copper and a zinc ion per each identical subunit.[1] The copper ion is coordinated to four histidine residues, one of them acting, as histidinato, as a bridge between the copper and the zinc ion. The coordination of zinc is completed by two other histidines and an aspartate residue. Copper is at the bottom of a wide channel bearing numerous charged groups, which can have a relevant role in the catalytic mechanism. The protein has a molecular weight of 32000.

The physiological role of SOD is the dismutation of superoxide radicals which are produced during the oxygen metabolic cycle and result to be extremely reactive toward the cells.[2] Superoxide is dismutated to molecular oxygen and to hydrogen peroxide,[3-7] which is then scavenged by other enzymes, like catalase. The catalytic mechanism occurs through a two-step process in which the copper ion is alternatively reduced, with the formation of molecular oxygen, and oxidized back to the resting state with production of hydrogen peroxide:[3,4,8]

$$\text{SOD-Cu}^{2+} + \text{O}_2^- \rightarrow \text{SOD-Cu}^{+} + \text{O}_2$$

$$\text{SOD-Cu}^{+} + \text{O}_2^- + 2\text{H}^+ \rightarrow \text{SOD-Cu}^{2+} + \text{H}_2\text{O}_2$$

The observed catalytic rates for this enzyme are very fast, of the order of $2\text{–}3 \times 10^9\ \text{s}^{-1}\ \text{M}^{-1}$, and are diffusion controlled.[4] Some of the residues present in the active channel have been shown, by studies on mutants obtained through site-directed mutagenesis, to play an important role in the structural and catalytic properties of the enzyme.[9-15] Among the residues that form the active site channel, i.e., Arg 143, Thr 58, Thr 137, Lys 136, Glu 132, and Glu 133, the most relevant, in terms of enzymatic behavior, is Arg 143,[9,10] which is invariant among the SOD enzymes for which the primary structure has been determined.[16] In this paper, we use the residue numbering of the human isoenzyme, even if the structure is available for the bovine isoenzyme,[1] as all the studies on the mutants have been performed, up to now, on the human isoenzyme.

When Arg 143, which is positively charged at physiological pH, is substituted by a neutral group or, more, by a negative group, the catalytic rates of SOD decrease by one to two orders of magnitude, without any major perturbation of the metal ion ligands.[9,10]

SOD has been the object of a large number of computational studies which tried to rationalize different aspects of its enzymatic behavior.[17-24] The fundamental role played by the electrostatic interactions in the catalytic activity of SOD has been investigated and discussed in a large number of experimental[25-27] and theo-

* Mailing address: Prof. Lucia Banci Department of Chemistry, University of Florence, Via G. Capponi 7, 50121 Florence, Italy.

(1) Tainer, J. A.; Getzoff, E. D.; Beem, K. M.; Richardson, J. S.; Richardson, D. C. *J. Mol. Biol.* **1982**, *160*, 181–217.
(2) (a) Fridovich, I. *Adv. Enzym.* **1974**, *41*, 35. (b) Fridovich, I. *Adv. Enzym. Relat. Areas Mol. Biol.* **1986**, *58*, 61–97.
(3) Mc Cord, J. M.; Fridovich, I. *J. Biol. Chem.* **1969**, *244*, 6049–6055.
(4) Fee, J. A.; Bull, C. *J. Biol. Chem.* **1986**, *261*, 13000–13005.
(5) (a) Fee, J. A. In *Metal Ions in Biological Systems*; Sigel, H., Ed.; M. Dekker: New York, 1981, Vol. 13, pp 259–298. (b) Fee, J. A, *In Metal Ion Activation of Dioxygen*; Spiro, T. G., Ed.; Wiley: New York, 1980; pp 209–327. (c) Fee, J. A. In *Oxygen and Oxy-Radicals in Chemistry and Biology*; Rodgers, M. A. J., Powers, E. L., Eds.; Academic Press: New York, 1981; pp 204–221, 221–239.
(6) Valentine, J. S.; Pantoliano, M. W. In *Metal Ions in Biological Systems*; Sigel, H. Ed.; M. Dekker: New York, 1981; Vol. 3, pp 291–358.
(7) Banci, L.; Bertini, I.; Luchinat, C.; Piccioli, M. *Coord. Chem. Rev.* **1990**, *100*, 67–103.
(8) Tainer, J. A.; Getzoff, E. D.; Richardson, J. S.; Richardson, D. C. *Nature (London)* **1983**, *306*, 284–287.
(9) Beyer, W. F.; Fridovich, I.; Mullenbach, G. T.; Hallewell, R. A. *J. Biol. Chem.* **1987**, *23*, 11182–11187.
(10) Banci, L.; Bertini, I.; Luchinat, C.; Hallewell, R. A. *J. Am. Chem. Soc.* **1988**, *110*, 3629–3633.
(11) Banci, L.; Bertini, L.; Luchinat, C.; Hallewel, R. A. *Ann. N.Y. Aca. Sci.* **1988**, *542*, 37–52.
(12) (a) Bertini, I.; Banci, L.; Luchinat, C.; Bielski, B. H. J.; Cabelli, D. E.; Mullenbach, G. T.; Hallewell, R. A. *J. Am. Chem. Soc.* **1989**, *111*, 714–719. (b) Banci, L.; Bertini, I.; Cabelli, D. E.; Hallewell, R. A.; Luchinat, C.; Viezzoli, M. S. *Inorg. Chem.* **1990**, *29*, 2398–2403.
(13) Bertini, L.; Banci, L.; Turano, P. *Eur. Biophys. J.* **1991**, *19*, 141–146.
(14) Banci, L.; Bertini, I.; Cabelli, D. E.; Hallewell, R. A.; Luchinat, C.; Viezzoli, M. S. *Free Radical Research Commun.* **1991**, *12–13*, 239–251.
(15) Getzoff, E. D.; Cabelli, D. E.; Fisher, C. L.; Parge, H. E.; Viezzoli, M. S.; Banci, L.; Hallewell, R. A. *Nature*, in press.
(16) Getzoff, E. D.; Tainer, J. A.; Stempien, M. M.; Bell, G. I.; Hallewell, R. A. *Proteins: Struct. Funct., Gen* **1989**, *5*, 322–366.
(17) Osman, R.; Bash, H. *J. Am. Chem. Soc.* **1984**, *106*, 5710–5714.
(18) (a) Rosi, M.; Sgamellotti, A.; Tarantelli, F.; Bertini, I.; Luchinat, C. *Inorg. Chim. Acta* **1985**, *107*, L21–L22. (b) Rosi, M.; Sgamellotti, A.; Tarantelli, F.; Bertini, I.; Luchinat, C. *Inorg. Chem.* **1986**, *25*, 1005–1008.
(19) Getzoff, E. D.; Tainer, J. A.; Weiner, P. K.; Kollman, P. A.; Richardson, J. S.; Richardson, D. C. *Nature (London)* **1983**, *306*, 287–290.
(20) (a) Klapper, I.; Hagstrom, R.; Fine, R.; Sharp, K.; Honig, B. *Proteins: Struct. Funct. Gen.*, **1986**, *1*, 47–59. (b) Sharp, K.; Fine, R.; Honig, B. *Science* **1987**, *236*, 1460–1463.
(21) Head-Gordon, T.; Brooks, C. L., III *J. Phys. Chem.* **1987**, *91*, 3342–3349.
(22) (a) Allison, S. A.; McCammon, J. A. *J. Phys. Chem.* **1985**, *89*, 1072–1074. (b) Bacquet, R. J.; McCammon, J. A.; Allison, S. A. *J. Phys. Chem.* **1988**, *92*, 7134–7141.
(23) Sines, J. J.; Allison, S. A.; McCammon, J. A. *Biochemistry* **1990**, *29*, 9403–9412.
(24) Fisher, C. L.; Tainer, J. A.; Pique, M. E.; Getzoff, E. D. *J. Mol. Graphics* **1990**, 125–132.
(25) Malinowski, D. P., Fridovich, I. *Biochemistry* **1979**, *18*, 5909–5917.
(26) Cudd, A.; Fridovich, I. *J. Biol. Chem.* **1982**, *257*, 11443–11447.

0002-7863/92/1514-6994$03.00/0

retical[19-24] articles. Particularly, electrostatic potential calculations and Brownian dynamics simulations on wild type (WT)[19-22] and mutated SOD[23] suggested that the most dramatic effect is due to a few key residues only (Arg 143, Glu 133, Lys 136); in particular, the calculations performed on a system in which the charge of Arg 143 had been neutralized or, even more, reversed provided reduced catalytic rates as experimentally observed. A recent paper,[24] making use of normal mode analysis, reported the effects of protein flexibility on electrostatic recognition of the substrate.

Molecular dynamics calculations (MD)[28-31] can be of invaluable importance in order to understand the dynamics of the active site channel in this enzyme, which can be relevant for the recognition of substrate and for the different steps of the catalytic pathway. In addition, MD calculations can be useful in order to understand how the active cavity and the channel are perturbed upon substitution of specific residues. Finally, the dynamic behavior of residue–residue interactions, which can play a key role in the catalytic mechanism, can be successfully addressed by MD calculations.

For these reasons we have undertaken MD studies on SOD, both WT and mutants in which the Arg 143 group is substituted by either a Glu or an Ile. We have started by building a set of parameters which correctly model the metal sites in SOD and which made us confident in the results of the MD trajectories on the various systems investigated here. Then trajectories on WT and some of its mutants, already experimentally characterized,[9,10] have been performed, and the structural changes and the fluctuations are discussed in terms of their relevance for the catalytic activity.

A MD study had been already reported on WT SOD,[32] which analyzed the fluctuations of the active channel. However, in that paper, aimed to the study of the diffusion motion of superoxide in the active channel, a less detailed determination of the parameters of the metal sites was used and a shorter trajectory on the WT was calculated, which did not allow the analysis of group fluctuations which can occur on a larger time scale. While submitting the present paper, a subsequent, detailed MD study on WT SOD,[33] with a longer trajectory, appeared. In that paper, MD simulations were used to study the equilibrium distribution of a superoxide molecule in the active site channel of SOD.

The importance of the mobility of the active channel has been already proposed in the latter report[33] as well as in previous theoretical studies on SOD.[24,32]

Our goal here is that of analyzing the role of the various residues in the study of the dynamic behavior of mutants of SOD that will be then correlated with their experimental enzymatic behavior.

Computational Procedure

The entire simulation was carried out using the AMBER 3.A[34] program running on a IBM RS/6000 520 computer.

Protein Models. The asymmetric unit of bovine Cu_2Zn_2SOD contains two protein molecules, each of them being formed by two identical subunits.[1] We selected the coordinates of the molecule formed by the "orange" and "yellow" subunits, as reported in the Protein Data Bank file (2SOD). The X-ray structure has a resolution of 2 Å. Each subunit contains 151 amino acids, corresponding to 1086 heavy atoms, plus a copper and a zinc ion. On the basis of recent refinements of the X-ray structure, the OH group of Thr137, which in the Protein Data Bank structure is pointing toward copper, is found to interact with Glu133.[8,15] We therefore applied a 180° rotation of the $-CH\beta\langle^{C\gamma H_3}_{O\gamma H}$ group around the Cα–Cβ bond of Thr137, in order to reproduce the new structural properties. In addition, new coordinates for the two water molecules close to copper, with copper–water oxygen distances of 2.8 and 3.3 Å,[8,35] were used. We shall refer to these water molecules as "close water" (CWAT) and "far water" (FWAT) in the Results section. As far as the histidines are concerned, those bound to the metals were taken as neutral, except His 63 which was taken as deprotonated, in agreement with NMR studies on both reduced protein[36] and on the cobalt(II)-substituted derivative.[37] Regarding the two other histidine residues present in each subunit, His 20 was taken as neutral, as proposed in the X-ray structure paper,[1] with the hydrogen on the Nδ2 atom, as Nδ2 is weakly interacting with the carboxylate group of Glu 23. His 43 was set positive, protonated on both nitrogen atoms, accordingly to the H-bond patterns reported in the X-ray structure paper.[1] The hydrogen atoms were added through the EDIT module of AMBER. Since the overall charge of oxidized SOD is −4 at physiological pH, in order to neutralize the whole system, four sodium ions far from the active sites were added with the CION option of EDIT, avoiding to eventually break salt bridges among residues. They were located close to Asp 243, Asp 278, Asp 229, and immersed in the water, nearby Asp 278, i.e., all close to residues of the "yellow" subunit. Finally, the whole system was surrounded by a sphere of Monte Carlo TIP3P[38] waters with the SOL-BLOB option of the EDIT module of AMBER. The water molecules whose oxygen atom or hydrogen atoms are at 2.8 and 2.0 Å, respectively, from any protein atom were discarded. A BLOB thickness of 10 Å was chosen. The total water molecules were about 3300 for all the proteins here investigated; the resulting systems were composed by ≃13 200 atoms.

The mutated proteins were constructed with the use of the interactive computer graphics package SYBYL,[39] by simply replacing Arg 143 residue in the WT with a glutamate and an isoleucine. The backbone coordinates for these amino acids were not changed, and the residue side chains were located close to the side chain of Arg 143. Tests were made also by placing the side chains with slight different positions. No significant changes in the results were obtained. In the Glu143 mutant, the two additional sodium ions were added close to the two terminal Lys residues, while in the Ile 143 mutant only a sodium ion close to the terminal Lys residue of the "orange" subunit was added.

Charges and Force Field Parameters. The standard AMBER charges were used for all the atoms except for the residues of the active site (His 46, His 48, His 63, His 71, His 80, Asp 83, His 120, Zn and Cu), for which we used ab initio charges already reported in the literature.[40] AMBER all-atom force field parameters[41] were used for all the residues with, at least, one atom within a 15-Å sphere centered on Cu of the "orange" monomer. For the residues outside this sphere we used the united-atom parameters.[42] We chose this mixed set of parameters, which is a quite common procedure,[43] as it follows a better description of a large region around the metal sites, with the explicit inclusion of the hydrogen atoms, without an additional severe computational cost. The

(27) Argese, E.; Viglino, P.; Rotilio, G.; Scarpa, M.; Rigo, A. *Biochemistry* **1987**, *26*, 3224–3228.
(28) McCammon, J. A.; Harvey, S. C. *Dynamics of Proteins and Nucleic Acids*; Cambridge University Press: Cambridge, 1987.
(29) Brooks, C. L., III; Karplus, M.; Pettitt, B. M. *Proteins: A Perspective of Dynamics, Structure, Thermodynamics*; J. Wiley and Sons: New York, 1988.
(30) Kollman, P. A.; Merz, K. M., Jr. *Acc. Chem. Res.* **1990**, *23*, 246–252.
(31) van Gunsteren, W. F.; Berendsen, H. J. C. *Angew. Chem., Int. Ed. Engl.* **1990**, *298*, 992–1023.
(32) Shen, J.; Subramanian, S.; Wong, C. F.; McCammon, J. A. *Biopolymers* **1989**, *28*, 2085–2096.
(33) Shen, J.; McCammon, J. A. *Chem. Phys.* **1991**, *158*, 191–198.
(34) Singh, U. C.; Weiner, P. K.; Caldwell, J.; Kollman, P. A. AMBER 3A; San Francisco, 1986. Seibel, G. L. Revision A; University of California, San Francisco, 1989.
(35) D. Richardson, personal communication.
(36) Bertini, I.; Capozzi, F.; Luchinat, C.; Piccioli, M.; Viezzoli, M. S. *Eur. J. Biochem.* **1991**, *197*, 691–697.
(37) Banci, L.; Bertini, L.; Luchinat, C.; Piccioli, M.; Scozzafava, A.; Turano, P. *Inorg. Chem.* **1989**, *28*, 4650–4656.
(38) Jorgensen, W. L.; Chandrasekhar, J.; Madura, J.; Impey, R. W.; Klein, M. L. *J. Chem. Phys.* **1983**, *79*, 926–935.
(39) SYBYL, Molecular Modeling Software Package, Version 5.2, Tripos Associates Inc.
(40) Shen, J.; Wong, C. F.; Subramaniam, S.; Albright, T. A.; McCammon, J. A. *J. Comp. Chem.* **1990**, 346–350.
(41) Weiner, S. J.; Kollman, P. A.; Nguyen, D. T.; Case, D. A. *J. Comp. Chem* **1986**, *7*, 230–252.
(42) Weiner, S. J.; Kollman, P. A.; Case, D. A.; Singh, U. C.; Ghio, C.; Alagona, G.; Profeta, S., Jr.; Weiner, P. *J. Am. Chem. Soc.* **1984**, *106*, 765–784.
(43) Dagget, V.; Brown, F.; Kollman, P. A. *J. Am. Chem. Soc.* **1989**, *111*, 8247–8256. Vedani, A.; Hutha, D. W. *J. Am. Chem. Soc.* **1990**, *112*, 4759–4767. Merz, K. M. *J. Am. Chem. Soc.* **1991**, *113*, 3572–3575.

disulfide bond involving Cys 55 has been treated with the force field parameters of the standard AMBER database.[34]

Metal Dependent Parameters. It should be pointed out that, when one deals with systems containing transition metal ions, no standard force fields are available; in fact, even though several force fields for metal ions have recently been developed,[44,45] there is the fundamental problem that they are able to describe adequately a very narrow spectrum of metal environments, i.e., they can be used only for certain sets of ligands and for a well specified stereochemistry of the binding sites. Furthermore, many of these force fields, among which are those for Cu(II),[45] do not consider both the interaction with water and an explicit Coulomb interaction, as they are suited for small complexes; nevertheless, the latter interactions are usually essential to reproduce the behavior of biological systems. This is especially true for SOD, since it has been demonstrated that electrostatics play a crucial role in the interaction between the enzyme and the substrate.[19-23] On the basis of the above considerations, we decided to model both metal ions and their ligands in the active site by using the force field parameters recently developed by Merz et al.[46,47] for the zinc ion and its ligands in the active site of carbonic anhydrase (CA). These parameters, which consider both electrostatic and water interactions, resulted to be well suited for describing the dynamic properties of CA[46-48] and carboxypeptidase A (CPA).[49] The same parameters were used to model the copper and zinc coordination (i.e., metal ions and their ligands) in SOD. The equilibrium values for the bond and angle potentials were set according to the X-ray structure. No bond nor any distance constraint was set between the copper ion and the closest semibound water (CWAT) during the MD simulations. This choice is made in agreement with the results of angular overlap calculations on SOD,[50] which indicated that the coordination properties of copper on SOD can be described without taking the water molecule as a ligand. As far as the Asp–zinc bond is concerned, a distance constraint with a force constant of 20 kcal and an equilibrium distance value of 1.91 Å was introduced between an oxygen atom of Asp 83 (Oδ1) and the zinc ion, following a procedure already reported for describing the coordination of Glu 72 to zinc in CPA.[49] This parameter setup resulted in our systems being able to reproduce the structure of the active site which does not undergo any appreciable distortion during the dynamics (See Results section).

Molecular Dynamics Calculations. MD simulations for the WT, Glu 143 SOD, and Ile 143 SOD were carried out, with a residue-based cut-off value for the evaluation of pair interactions of 10 Å. The number of pair interactions during the MD simulations was about 2.1×10^6. The timestep of the dynamics was 1.5 fs, and a value of the dielectric constant of 1 was chosen. The pairlist was updated every 10 steps, and the values of the energies and the coordinates were saved every 100 steps. All the water molecules present in the system and the sodium ions were equilibrated by minimizing the rms energy gradient within 0.1 kcal mol^{-1} Å^{-1} followed by 9 ps of molecular dynamics. The two crystallographic water molecules found in the active site channel of each subunit were constrained in their starting position, only during the equilibration, by means of a harmonic potential of 0.5 kcal mol^{-1} Å^{-2}. The water and ion equilibration was followed by the energy minimization of the whole protein molecule, in which 3300 steps of steepest descent method proceeded until the convergence condition (energy gradient $\leq$0.1 kcal mol^{-1} Å^{-1}) was met. Then, molecular dynamics simulations were performed for 63 ps on the atoms within a 26-Å sphere around copper in the "orange" subunit. This choice included in the dynamics all the atoms of the "orange" subunit and the atoms of the "yellow" subunit at the subunit–subunit interface. The total number of atoms included in the dynamics was 6536 for WT, 6562 for Arg 143 → Glu mutant, and 6372 for Arg 143 → Ile mutant. The whole system was coupled to a thermal bath[51] of $T = 300$ K with a relaxation time of 0.2 ps. During the MD simulations, bond lengths were constrained to equilibrium values using the SHAKE[52] algorithm. The water molecules in the shell between 20 and 26 Å from the copper ion were constrained to a harmonic potential around their initial position (force constant = 0.5 kcal mol^{-1} Å^{-2}). This would prevent their evaporation without affecting their motion, due to the very low force constant.

Data Analysis. The coordinates of the last 36 ps (27–63 ps) were used for structural analysis. Averaged structures were calculated for the protein atoms using the MDANAL module of AMBER.[34] The appropriate geometry of the residues is fairly maintained in the average structure, except for the water molecules and the CH_3 groups which were not taken into account in the rms analysis. The root mean square (rms) fluctuations at the time t_s, averaged over the protein atoms involved in the MD and over time, from the starting time step ($t_j = 27$ ps) to the sth time step ($t_j = t_s$) were calculated as

$$\left\{\frac{1}{n}\sum_{i=1}^{n}\frac{1}{s}\sum_{j=1}^{s}|r_i(t_j) - \langle r_i\rangle|^2\right\}^{1/2}$$

where r_i is the position of the ith atom, t_j the jth timestep, and n the total number of atoms. The rms deviations of the average structure with respect to the X-ray structure were calculated as $(\sum_{i=1}^{n}|\Delta r_i|^2/n)^{1/2}$ where Δr_i is the displacement of an atom in the average MD structure with respect to the X-ray structure, and the sum is performed over all the atoms in a residue (deviation per residue) or over all the atoms in the protein (deviation of the entire structure).

Results and Discussion

All the analysis of trajectories refers to the behavior of the "orange" subunit.

The Active Site. In Table I, distances and angles between the two metal ions and the atoms of their ligands as well as of some relevant groups in the cavity are reported for the starting (X-ray) structure, the minimized one, and the structure obtained after 18 ps of dynamics, for which the total energy is constant for WT SOD. In addition, the absolute deviations for those distances and angles are reported.

As it can be seen, the geometry of the metal sites and some important interactions are maintained, thus indicating that the set of parameters we built for the metal ions and their ligands is phenomenologically reliable for studying the dynamics of this molecule. This procedure for checking the parameters of the metal ion and of its ligands has been proposed and successfully used by Merz et al. on the enzyme CA.[48] We would like to stress here that the present paper is focused on the analysis of the motions of the active channel, in relation to their enzymatic relevance, rather than on the coordination geometry of the metal ions.

Table I reports distances and angles for the two metal sites and also for further steps of the trajectory. It can be seen that the metal sites structure is fairly maintained.

MD on WT SOD. After a few picoseconds of equilibration, the total energy of the system as well as the potential and kinetic energies become constant, showing only small fluctuations. In the present run, the averaged rms fluctuation over all the atoms of the "orange" subunit is 0.57 Å, while on its backbone atoms

(44) (a) Hay, B. P. *Inorg. Chem.* **1991**, *30*, 2876–2884 and references therein. (b) Hancock, R. D.; Dobson, S. M.; Boeyens, J. C. A. *Inorg. Chim. Acta* **1987**, *133*, 221–231. (c) Hancock, R. D.; Ngwenya, P. W.; Evers, A.; Wade, P. W.; Boeyens, J. C. A. *Inorg. Chem.* **1990**, *29*, 264–270. (d) Hancock, R. D. *Progr. Inorg. Chem.* **1989**, 187.

(45) (a) Brubaker, G. R.; Johnson, D. W. *Inorg. Chem.* **1984**, *23*, 1591–1595. (b) Brubaker, G. R.; Johnson, C. D. *Coord. Chem. Rev.* **1984**, *53*, 1. (c) Bernardt, P. V.; Comba, P., personal communication.

(46) Merz, K. M., Jr. *J. Am. Chem. Soc.* **1991**, *113*, 406–411.

(47) Merz, K. M., Jr.; Murcko, M.; Kollman, P. A. *J. Am. Chem. Soc.* **1991**, *113*, 4484–4490.

(48) Hoops, S. C.; Anderson, K. A.; Merz, K. M., Jr. *J. Am. Chem. Soc.* **1991**, *113*, 8262–8270.

(49) Banci, L.; Schroeder, S.; Kollman, P. A. *Proteins: Struct., Funct. Gen.* **1992**, *13*, 288–305.

(50) Banci, L.; Bencini, A.; Bertini, I.; Luchinat, C.; Piccioli, M. *Inorg. Chem.* **1990**, *29*, 4867–4873.

(51) Berendsen, H. J. C.; Postma, J. P. M.; van Gunsteren, W. F.; DiNola, A.; Haak, J. R. *J. Chem. Phys.* **1984**, *81*, 3684–3690.

(52) van Gunsteren, W. F.; Berendsen , H. J. C. *Mol. Phys.* **1979**, *34*, 1311–1327.

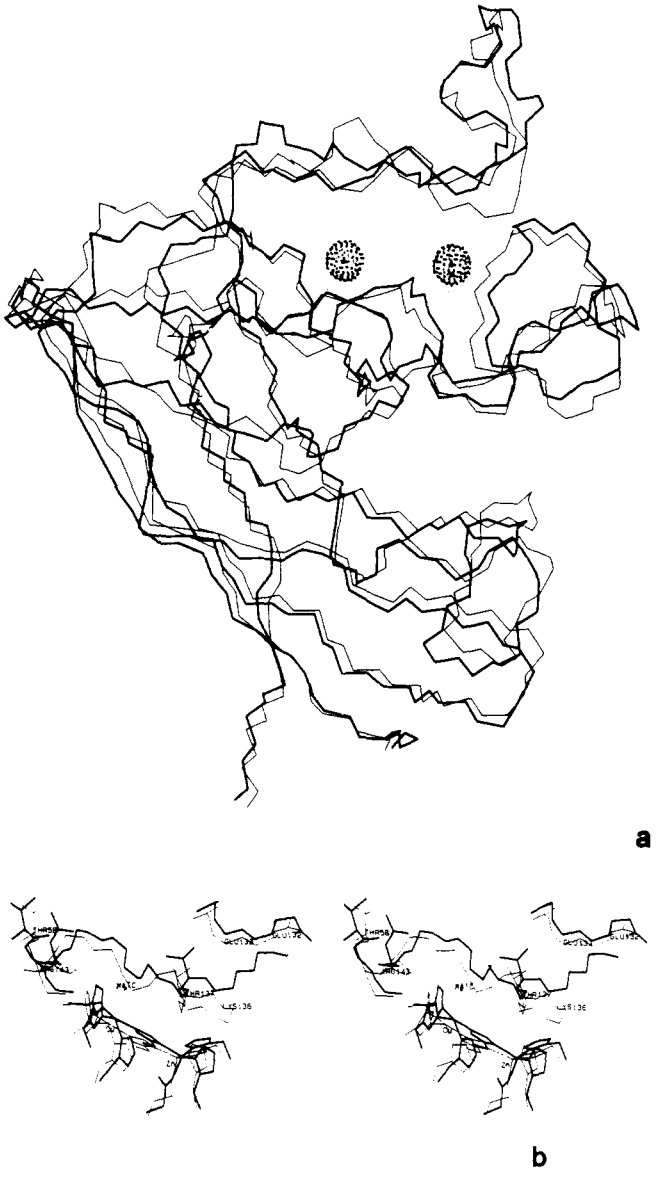

Figure 1. (a) Comparison between the backbone of the X-ray (thin line) and MD average (bold line) structures of WT SOD and (b) stereoview of the active site in the two structures. In (b) the most relevant residues, in addition to the ligands of the metal ions, are shown.

the fluctuation is 0.49 Å. The rms fluctuations become constant, on average, after 15–18 ps.

A MD average structure is generated and a comparison with the X-ray structure is reported in Figure 1, where the comparison of the two backbones is shown in Figure 1a and that of the metal sites, together with some relevant residues, is reported in Figure 1b. The rms deviation of the average MD structure with respect to the starting (X-ray) one is 1.53 Å, averaged over all the atoms, and 1.21 Å, averaged over the backbone atoms, while the rms deviation of the minimized structure with respect to the starting one is 0.73 Å, averaged over all the atoms, and 0.66 Å, averaged over the backbone atoms. Figure 2a reports the deviation (averaged per residue) between the X-ray and the MD average structure. Table II reports some relevant interatomic distances for the X-ray, minimized and MD average structures.

The overall structure of the protein is well maintained as shown in Figure 1a, even if the protein shows some flexibility. From all the above data, it is possible to locate some residues which have large fluctuations along the trajectory and which show large deviations, in the averaged structure, from the starting structure. The residues in the range 9–11, 47–55, 100–108, and 119–143 show a large mobility. Among these, it is important to note that the charged groups Arg 143, Glu 133, and Lys 136, present in

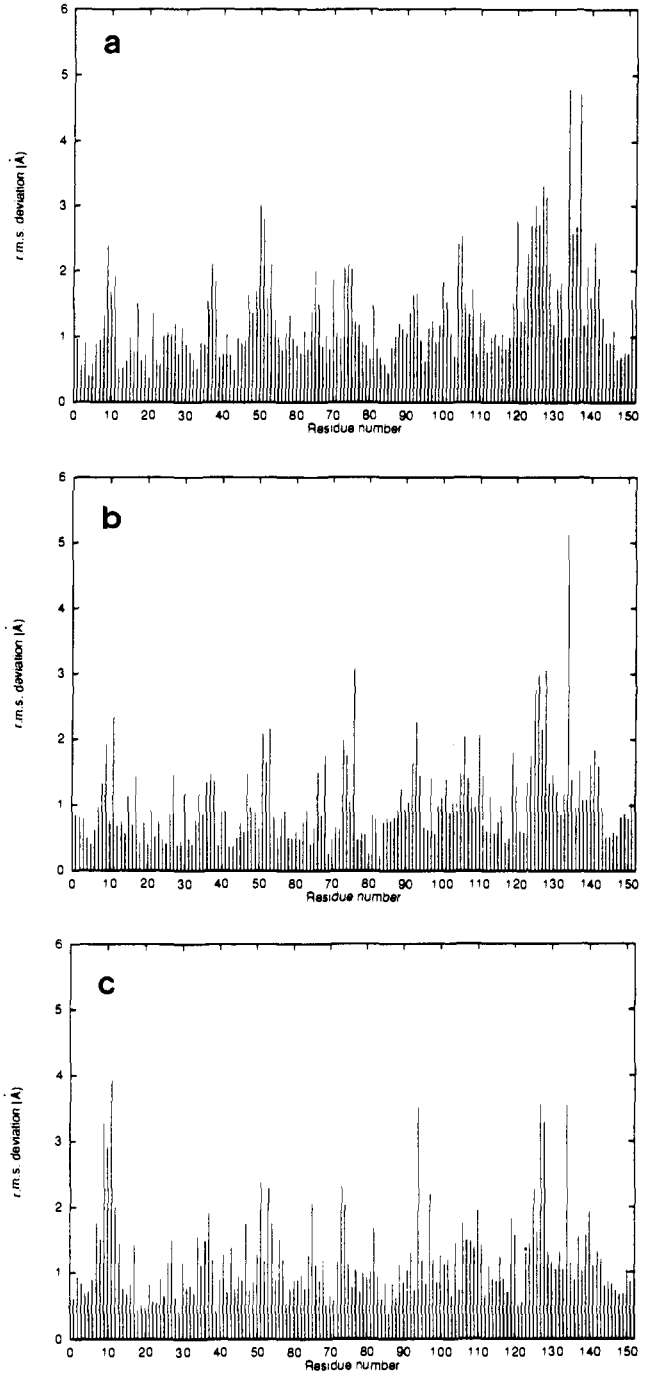

Figure 2. Rms deviation, averaged per residue, of the MD average structures with respect to the starting structures for (a) WT SOD, (b) Arg 143 → Glu SOD, (c) Arg 143 → Ile SOD.

the active site channel, experience a large movement during the dynamics.

Along the entire trajectory, the metal sites remain quite stable; even the second, long-range bridge formed by Asp 124, which is H-bonded to both His 46 and His 71, is fairly stable during the dynamics.

The bottleneck of the active site channel is quite flexible, and the width of the channel itself increases as the system is allowed to relax. Figure 3 shows the fluctuations of the distance between Cζ of Arg 143 and Cβ of Thr 137, the two groups which determine the narrowest section of the active channel. During the calculation the two groups move apart and the channel becomes wider, the movement being mostly due to Arg 143.

The guanidinium group of Arg 143, during the dynamics, rotates around the Cγ–Cδ bond. The guanidinium group is also slowly moving away from copper pointing toward the outside of

Table I. Distances and Angles between Metal Ion and Ligands and between Metal Ion and Selected Residues in WT SOD, for the X-ray and Minimized Structures and for the Structures After 18, 40, and 60 ps

	X-ray structure	minimized	deviation	18 ps	deviation	40 ps	deviation	60 ps	deviation
				distances (Å)					
Cu–Nδ1 (His46)	2.0	2.1	0.1	2.1	0.1	2.1	0.1	2.1	0.1
Cu–Nε2 (His48)	2.1	2.2	0.1	2.1	0.0	2.1	0.1	2.1	0.1
Cu–Nε2 (His63)	2.2	2.2	0.0	2.1	−0.1	2.1	−0.1	2.1	−0.1
Cu–Nε2 (His120)	2.1	2.1	0.0	2.1	0.0	2.1	0.1	2.1	0.1
Cu–O (CWAT)	2.8	2.2	−0.6	2.2	−0.6	2.7	−0.1	2.4	−0.4
Zn–Nδ1 (His63)	2.1	2.1	0.0	2.0	−0.1	2.0	−0.1	2.0	−0.1
Zn–Nδ1 (His71)	2.1	2.1	0.0	2.0	−0.1	2.0	−0.1	2.0	−0.1
Zn–Nδ1 (His80)	2.0	2.0	0.0	2.0	0.0	2.0	0.0	2.0	0.0
Zn–Oδ1 (Asp82)	1.9	1.9	0.0	2.0	0.1	1.8	−0.1	1.9	0.0
Oδ1 (Asp124)–Nε2 (His71)	2.4	2.6	0.2	2.7	0.3	3.1	0.7	2.9	0.5
Oδ2 (Asp124)–Nε2 (His46)	2.9	2.7	−0.2	3.1	0.2	2.8	−0.1	3.1	0.2
Cζ (Arg143)–Cu	5.6	6.3	0.7	7.2	1.6	7.8	2.2	7.9	2.3
Oγ1 (Thr137)–Cu	7.9	6.4	−1.5	9.0	1.1	7.9	0.0	9.4	1.5
				angles (deg)					
Nε2 (His120)–Cu–Nε2 (His48)	106.4	106.4	0.0	111.7	5.3	109.2	2.8	118.4	12.0
Nε2 (His120)–Cu–Nε2 (His46)	93.7	86.2	−7.5	89.8	−3.9	87.8	−5.9	84.0	−9.7
Nδ1 (His46)–Cu–Nε2 (His63)	74.7	79.6	4.9	78.4	3.7	85.7	11.0	81.7	5.3
Nε2 (His48)–Cu–Nε2 (His63)	89.1	87.3	−1.8	87.8	−1.3	89.0	−0.1	81.4	−7.7
Nε2 (His120)–Cu–Nε2 (His63)	164.5	165.0	0.5	160.2	−4.3	159.6	−4.9	159.0	−5.4
Nε2 (His48)–Cu–Nδ1 (His46)	130.2	135.4	5.2	132.9	2.7	135.0	4.8	145.8	15.6
Nδ1 (His63)–Zn–Nδ1 (His71)	111.1	111.8	0.7	114.5	3.4	111.4	0.3	114.0	2.9
Nδ1 (His63)–Zn–Oδ1 (Asp83)	100.0	116.5	16.5	90.6	9.4	112.5	12.5	91.0	−9.0
Nδ1 (His80)–Zn–Oδ1 (Asp83)	124.1	103.7	−20.4	128.1	4.0	115.2	−8.9	110.0	−14.1
Nδ1 (His80)–Zn–Nδ1 (His71)	130.0	122.3	−7.7	112.1	−17.9	115.8	−14.2	118.3	−11.7
Nδ1 (His71)–Zn–Oδ1 (Asp83)	78.7	91.2	13.2	99.9	21.1	95.9	17.2	95.3	16.6
Nδ1 (His63)–Zn–Nδ1 (His80)	107.5	109.6	2.1	110.2	2.8	106.2	−1.3	113.2	5.7

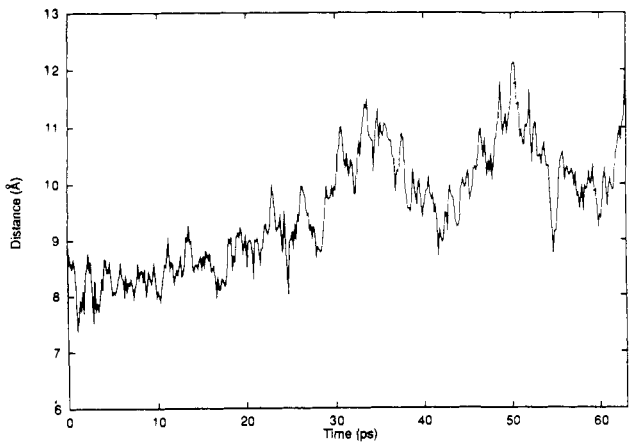

Figure 3. Fluctuations of the distance between Cζ Arg 143 and Cβ Thr 137 with WT SOD.

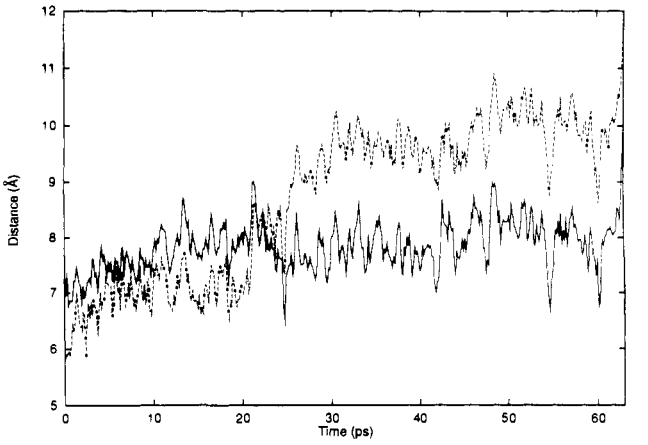

Figure 4. Fluctuations of the distance between copper and Nη1 Arg 143 (solid line) and copper and Nη2 Arg 143 (dashed line) in WT SOD.

the channel, even if a nitrogen atom is never too far from the copper ion (Figure 4).

The cavity is highly solvated; CWAT remains close to the copper ion along all the trajectory with an average Cu–O distance of 2.4 Å and an rms deviation of 0.2 Å, in good agreement with the experimental results obtained in solution from water relaxation measurements.[53] Thus, this water molecule is kept close to copper by nonbonded interactions that are strong enough to maintain a constant distance. This is a quite relevant result as it indicates that the set of parameters used for describing the metal ions are good and capable to reproduce even subtle experimental observations.

FWAT, on the contrary, is extremely mobile, interacting with Arg 143 and following this group during some steps of the simulation. When FWAT is not interacting with Arg 143, it is replaced by other water molecules which maintain the guanidinium group always highly solvated. The active site channel contains a large number of water molecules at its entrance, but the degree of solvation decreases getting closer to the copper ion; within 6.5 Å, on average, from the copper ion, only one water molecule, beside CWAT, is present.

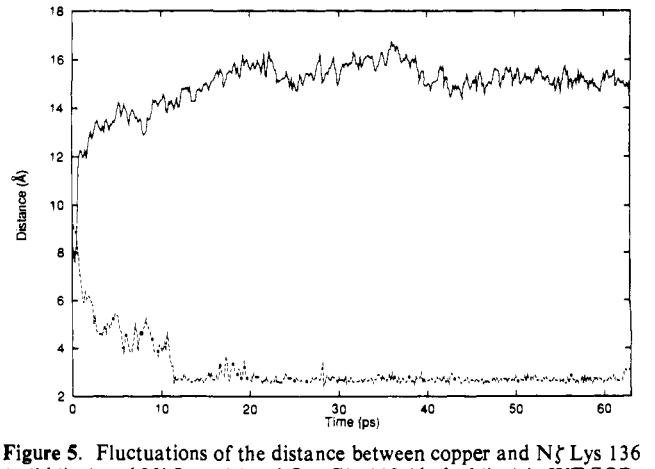

Figure 5. Fluctuations of the distance between copper and Nζ Lys 136 (solid line) and Nζ Lys 136 and Oε1 Glu 132 (dashed line) in WT SOD.

In the X-ray structure, Lys 136 is located on the opposite side of the active channel with respect to Arg 143 and close to the zinc

(53) Banci, L.; Bertini, I.; Hallewell, R. A.; Luchinat, C.; Viezzoli, M. S. *Eur. J. Biochem.* **1989**, *184*, 125–129.

Table II. Some Relevant Distances[a] for the Minimized and MD Averaged Structures of WT SOD, Arg 143 → Glu SOD, and Arg 143 → Ile SOD

		WT		Arg 143 → Glu		Arg 143 → Ile	
	X-ray structure	minimized	averaged	minimized	averaged	minimized	averaged
			Cu				
Cu–Oγ1 (Thr137)	7.9	7.4	8.6	7.5	6.8	7.8	7.0
Cu–Nζ (Lys136)	7.6	8.5	15.3	7.9	12.2	8.2	13.1
Cu–Oε1 (Glu133)	12.5	12.0	12.3	11.9	11.9	11.5	9.7
Cu–Oε2 (Glu133)	10.4	10.2	10.5	10.8	11.9	9.8	10.6
Cu–Oε1 (Glu132)	15.2	14.7	16.2	14.3	16.3	13.9	15.6
Cu–Oε2 (Glu132)	17.2	16.7	16.8	16.0	16.9	15.7	15.9
Cu–Nη1 (Arg143)	7.0	7.3	7.9				
Cu–Nη2 (Arg143)	5.1	6.1	9.8				
Cu–Oε1 (Glu143)	5.7[b]			6.8	5.1		
Cu–Oε2 (Glu143)	5.3[b]			5.4	6.7		
Cu–Cγ1 (Ile143)	6.2[b]					5.7	5.8
Cu–Cγ2 (Ile143)	6.3[b]					7.5	7.7
Cu–O (CWAT)	2.8	2.2	2.4	2.2	2.3	2.2	2.3
			Lys136				
Nζ–Oε1 (Glu132)	9.4	8.7	2.6	8.5	7.2	8.3	4.6
Nζ–Oε2 (Glu132)	11.0	10.7	4.0	10.1	8.7	9.6	5.0
Nζ–Oε1 (Glu133)	9.2	9.2	7.2	8.5	3.3	8.4	8.8
Nζ–Oε2 (Glu133)	8.2	8.7	8.5	8.5	3.3	8.2	7.9
Nζ–Oγ1 (Thr137)	6.0	5.8	7.8	5.1	5.9	5.0	8.6
Nζ–Zn	3.9	5.5	5.2	5.6	7.9	6.2	9.6
			Thr137				
Oγ1–Oε1 (Glu133)	5.2	5.3	4.0	5.1	5.2	4.7	3.2
Oγ1–Oε2 (Glu133)	3.6	4.3	2.9	4.9	5.2	4.0	4.1
Oγ1–Oε1 (Glu132)	7.9	7.5	8.4	7.0	10.3	6.1	9.5
Oγ1–Oε2 (Glu132)	9.9	9.5	9.6	8.7	11.0	8.0	9.9
Oγ1–O (CWAT)	6.1	5.7	6.4	6.0	4.6	6.2	4.9
			Arg143				
Nη1–Oγ1 (Thr137)	11.1	11.2	9.7				
Nη2–Oγ1 (Thr137)	9.4	8.9	11.6				
Cζ–Cβ (Thr137)	8.8	8.9	10.2				
Nη2–O (CWAT)	4.4	5.2	9.1				
			Glu143				
Oε1–Oγ1 (Thr137)	11.7[b]			11.8	7.2		
Oε2–Oγ1 (Thr137)	10.0[b]			9.6	8.8		
Cδ–Cβ (Thr137)	9.6[b]			9.6	7.6		
Oε2–O (CWAT)	4.4[b]			4.5	6.3		
			Ile143				
Cγ1–Oγ1 (Thr137)	10.9[b]					11.5	10.4
Cγ2–Oγ1 (Thr137)	12.2[b]					14.0	12.8
Cβ–Cβ (Thr137)	11.0[b]					11.8	10.7
Cγ2–O (CWAT)	6.3[b]					8.0	8.4

[a] Distances in Å. [b] These distances refer to the starting structure with the mutated aminoacid.

ion. During the dynamics Lys 136 undergoes large movements, moving away from copper (Figure 5, solid line) and interacting, after a few picoseconds of equilibration, with the negative carboxylate group of Glu 132 (Figure 5, dashed line). These two groups (Lys 136 and Glu 132) are conserved in most of the sequences known up to now.[17]

Glu 132 and Glu 133 are two negative groups at the entrance of the active site cavity which, on the basis of electrostatic calculations[20,23] and of experimental results[15] on mutants, produce a negative field which decreases the attraction for the substrate. The highly conserved Lys 136 group might have, on the basis of the present MD calculations, the role of neutralizing the negative groups of the highly conserved residues Glu 132 and Glu 133. In the present simulation, Lys 136 interacts with Glu 132, while the carboxylate group of Glu 133 is H-bonded to the OH moiety of Thr 137 (Oγ1–Oε2 distance is 2.9 Å on average). All these interactions determine an extensive H-bond net at the entrance of the channel which would induce the correct orientation of the charged groups for substrate diffusion toward the active site. Glu132 remains in a position similar to that observed in WT SOD but is not experiencing any significant interaction with residues closeby.

MD on Arg 143 → Glu SOD Mutant. The mobility of the active channel is decreased as a result of the substitution of the residue

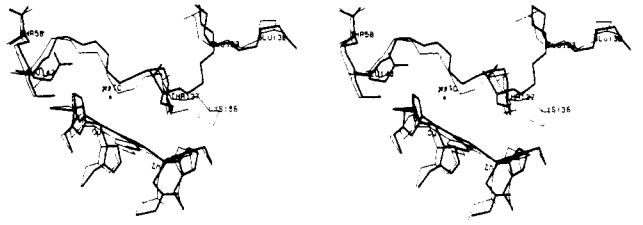

Figure 6. Stereoview of the active site in the starting (thin line) and MD average (bold line) structures of Arg 143 → Glu SOD. The most relevant residues, in addition to the ligands of the metal ions, are shown.

at the 143 position, while the overall mobility of the protein is similar to that of WT. The system equilibrates after a few picoseconds of dynamics. The average rms fluctuation of the "orange" subunit is 0.53 and 0.46 Å for the sole backbone. Again, the residues experiencing the largest fluctuations are those in the channel or near the active site. The mean deviation of the "orange" subunit between the MD average structure and the starting one is 1.26 Å for all the protein atoms and 0.93 Å for the backbone, while the values for the minimized structure with respect to the starting structure are 0.77 and 0.71 Å, respectively. The rms deviation averaged per residue is reported in Figure 2b. The largest

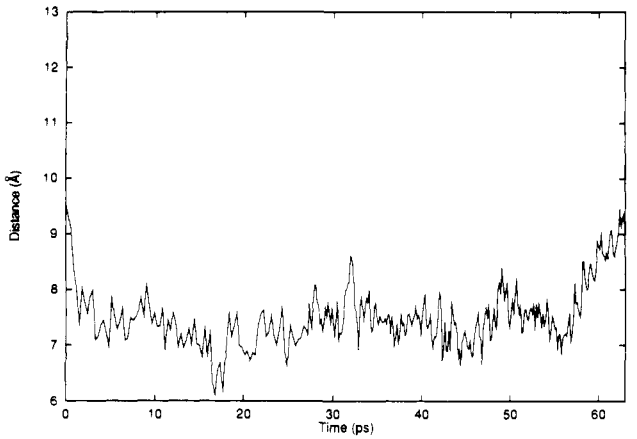

Figure 7. Fluctuations of the distance between Cδ Glu 143 and Cβ Thr 137 in Arg 143 → Glu SOD.

deviations are again for residues in the channel, yet at a smaller extent for the present case.

Figure 6 shows the comparison between the starting and the MD average structure for the active site residues. The metal site structure is maintained also in the present system, and the number of water molecules in the cavity is almost constant. CWAT stays close to copper, with an average Cu–O distance of 2.3 Å, with an rms of 0.3 Å. This finding is again in agreement with the experimental results.[53] FWAT, on the other hand, is quite mobile and diffuses out of the cavity.

The main feature of the present system is the reduced width of the active channel entrance: Glu 143 is attracted inside the cavity and toward the copper ion, while Arg 143 is not. This produces a very narrow bottleneck to the copper site. Figure 7 shows the distance between Cδ Glu 143 and Cβ Thr 137; the closest approach of the two residues, taking into account the complete side chain, could be as small as 5.5 Å. Lys 136 is extremely mobile also in the present system and, after a few ps, is H-bonded to Glu 133. The OH group of Thr 137 is also pointing toward Glu 133, even if it remains far for any kind of interaction.

MD on Arg 143 → Ile SOD Mutant. This system has a neutral, hydrophobic group on position 143, instead of the positively charged, hydrophilic arginine. This system has intermediate properties, from the electrostatic point of view, with respect to WT and Arg 143 → Glu SOD mutant. And indeed an intermediate behavior is observed in the MD trajectory with respect to the other investigated systems.

After a few picoseconds of equilibration, the system is fairly stable, with an average rms fluctuation of the "orange" subunit of 0.56 and of 0.50 Å for the backbone atoms. In agreement with what observed with the other two investigated systems, the largest fluctuations as well as the largest deviations are observed for residues in the active site channel. The deviation from the starting structure is smaller than for WT SOD, with an average rms deviation of 1.36 and of 1.15 Å for the backbone atoms. The rms deviation averaged per residue is reported in Figure 2c. The values of the rms fluctuations and rms deviations result, for this system, in an intermediate value between those of WT and those of Arg 143 → Glu SOD. Figure 8 shows the comparison of the active site channel for the starting and the MD average structure for Arg 143 → Ile SOD.

Also in this mutant the active site is quite stable, and the coordination geometry is maintained along the entire trajectory. In particular, the CWAT molecule stays close to the copper ion, with a copper–oxygen distance very similar to that found for the other two systems (2.32 Å with an rms deviation of 0.01 Å). This suggests that the nature of the residue on position 143 is not responsible for the presence of a semicoordinated water molecule at the copper ion. This, indeed, is again in agreement with the experimental results from NMRD measurements.[53]

Ile 143 has a quite stable position, with the Cβ Ile 143–Cβ Thr 137 distance remaining constant along the entire trajectory (Figure 9). It is interesting to note that, in the case of this mutant, which

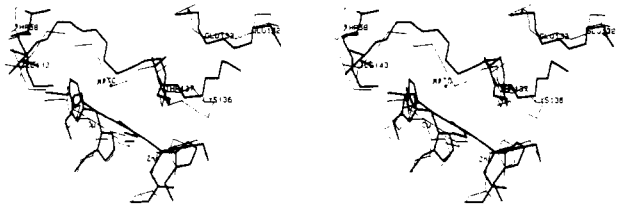

Figure 8. Stereoview of the active site in the starting (thin line) and MD average (bold line) structures of Arg 143 → Ile SOD. The most relevant residues, in addition to the ligands of the metal ions, are shown.

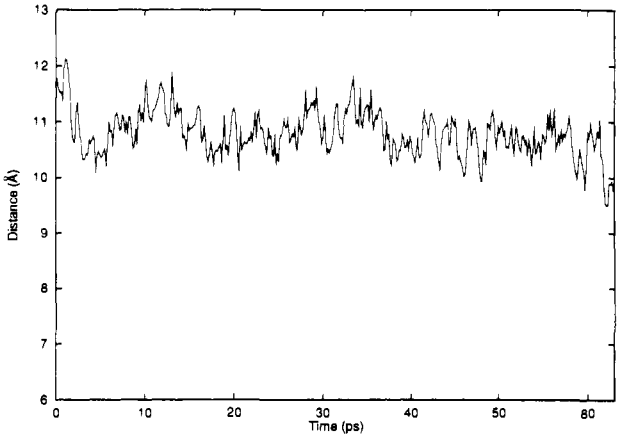

Figure 9. Fluctuations of the distance between Cβ Ile 143 and Cβ Thr 137 in Arg 143 → Ile SOD.

has on position 143 a neutral residue, the width of the channel remains very close to that of the starting structure. This result could be indicative of a further role of the positive group Arg 143. The positive group, located at this position, may have a relevant structural role, in addition to its fundamental electrostatic role, determining a large flexibility of the active site channel. The group at position 143 would behave as a "gate" which, depending on the nature of the residue, tends to open or to close the access to the substrate.

Glu 133 slightly approaches the copper ion and interacts with γOH Thr 137, while Lys 136 interacts with Glu 132, obtaining Nζ1 Lys 136–Oε1 Glu 132 distances as low as 2.5 Å at the end of the trajectory. The rearrangement of Lys 136 is similar to that observed for WT SOD, providing similar structures for the two systems; however, in the present case, the rearrangement occurs at longer simulation time. These results indicate that the Glu 132–Glu 133–Lys 136–Thr 137 side chains establish similar interactions in all the systems investigated. These residues form quite a stable network which can have an important role in the enzymatic catalysis from both the electrostatic and the structural point of view.

Implications for the Mechanism

Our results have shown that MD calculations may be an appropriate tool for the characterization of SOD, as they allow a detailed study of the mobility of the residues in the channel and of their role in the enzymatic catalysis.

The rate limiting step for the catalytic process in SOD is, in nonsaturating concentrations of the substrate, as it occurs at physiological pH, the diffusion of the substrate in the active site channel and its binding to the copper ion.[4]

The Arg 143 → Ile and Arg 143 → Glu SOD mutants experience a decrease of biological activity (about 10% and 4–2% of the WT activity, respectively)[10] as well as a parallel decrease in the affinity for small anions, like azide, which can simulate the substrate.[10]

The high catalytic rates of SOD are strongly determined by electrostatic effects which attract the substrate to the active site. This has already been demonstrated by electrostatic potential calculations[19–23] as well as by experimental work.[10,15] The present

MD calculations, however, show that other factors could contribute to the efficiency of the enzyme. Indeed, the dynamics of the cavity can be important for increasing the affinity of SOD toward the substrate. In WT SOD, the active site cavity has a large mobility, and the surface exposed to the solvent, and therefore to the substrate, is larger than that observed in the crystallographic structure. This suggests a synergistic role for the active cavity, where the electrostatic effects are enhanced by the fluxionality of the cavity. The charged groups, due to their high mobility, could produce a large attraction for superoxide; the larger surface exposed to the solvent facilitates the entrance of O_2^-.

The relevance of structural fluctuations in ligand and substrate binding to proteins, especially if they are small molecules like in the present case, has been already extensively discussed.[28] A striking example of the effect of protein mobility in molecular binding is represented by myoglobin: energy calculations[54] have demonstrated that the CO and O_2 binding are strongly affected by the protein atoms fluxionality which determines the possible binding paths for these ligands in entering and leaving the heme pocket. The energy barriers for these paths are sizably reduced by protein motions. If myoglobin rigidly maintained its X-ray structure, no energetically feasible path was possible.

The additional role for the active site channel due to its fluxionality is speculative at the present stage of the investigation but is consistent with the behavior of the two mutants here investigated. The reduced catalytic rates of the Arg 143 → Glu mutant correlate, in addition to the electrostatic effect of a negative charge, also with a reduced mobility and a smaller open section of the active site channel. The Arg 143 → Ile mutant, in which the positive charge is neutralized and not reversed in sign, has intermediate activity rates and intermediate mobility and open section of the channel, between the WT and the Arg 143 → Glu SOD mutant. Therefore, the group on the 143 position may behave like a "gate keeper" at the reaction site.

The mobility of other residues in the channel is directly connected with their involvement in the catalytic process. For example, the equilibrium position of Lys 136 results to be far from the copper ion, pointing outside the channel. Deprotonation of this residue was invoked as resposible of the drop in activity at high pH;[55] however a biophysical and biochemical characterization of proteins with residue 136 mutated to neutral, not ionizable, residues has shown that Lys 136 has only a small electrostatic effect, without affecting sizably the overall enzymatic behavior.[56] This finding is in complete agreement with our results from MD calculations.

The present MD simulations provide further hints on the enzymatic behavior of SOD and can shed light on the role of the active site channel in determining the high efficiency of this enzyme.

Acknowledgment. The authors are grateful to Prof. Ivano Bertini for his encouragement and helpful discussions. We wish to thank also Prof. Kenneth M. Merz, Jr., for his precious suggestions and comments on the manuscript.

(54) Case, D. A.; Karplus, M. *J. Mol. Biol.* **1978**, *132*, 343-368.

(55) O'Neil, P.; Davies, S.; Fielden, E. M.; Calabrese, L.; Capo, C.; Marmocchi, F.; Natoli, G.; Rotilio, G. *Biochem. J.* **1988**, *251*, 41.

(56) Banci, L.; Bertini, I.; Luchinat, C.; Viezzoli, M. S. Submitted.

Enantioselective Total Synthesis of (−)-Decarbamoylsaxitoxin

Chang Yong Hong and Yoshito Kishi*

Contribution from the Department of Chemistry, Harvard University, 12 Oxford Street, Cambridge, Massachusetts 02138. *Received November 7, 1991*

Abstract: An enantioselective total synthesis of (−)-decarbamoylsaxitoxin (**2**) has been accomplished, using the asymmetric trimolecular cyclization of **6**, i.e., **6** + (*R*)-glyceraldehyde 2,3-acetonide + $Si(NCS)_4$ → α-**7**, as the key step. The structure of the major product α-**7** was determined by X-ray crystallographic analysis, with the C-6 configuration corresponding to the unnatural antipode of decarbamoylsaxitoxin. Acetonide α-**7** was converted to thiourea **5**, an intermediate used in our previous racemic synthesis of saxitoxin. Thiourea **5** was further transformed to the tricyclic urea–thiourea **3**. At this stage, the ^1H NMR spectrum ($CDCl_3$) of optically active **3** was found to be dramatically different from that of racemic **3**. On the basis of concentration-dependent NMR spectroscopy and other studies, it was suggested that racemic **3** exists as a dimer of *d,l* pairs via two sets of hydrogen bonds whereas optically active **3** exists as a monomer because of a lack of such interactions due to geometric restriction. By following the previous synthetic route, tricyclic urea–thiourea **3** was converted to the unnatural antipode of decarbamoylsaxitoxin (**2**). Since the transformation of racemic, as well as optically active, decarbamoylsaxitoxin to saxitoxin has already been established, this synthesis constitutes a formal enantioselective total synthesis of saxitoxin. In addition, it was unambiguously demonstrated that the unnatural antipode of decarbamoylsaxitoxin exhibits no sodium channel blocking activity.

Introduction

The highly toxic nature of the red tide has been known and feared since ancient times. Periodic outbreaks of the red tide often occur during the summer months along the North Atlantic coasts of America and Europe, in particular along the North Pacific coast from California to Alaska, and the coastal areas of Japan and South Africa. Under certain tropical conditions, a toxic single-cell dinoflagellate *Gonyaulax catanella* grows at an abnormal rate. As these algae produce a red pigment(s), a bloom of dinoflagellates imparts a red color to the sea. Clams and mussels, feeding on these and other dinoflagellates by filtration of seawater through their siphon, concentrate the toxic principle of dinoflagellates in their organs and become poisonous to man, causing paralytic shellfish poisoning.[1]

In 1957, the toxic component of the paralytic shellfish poison was first isolated in the pure state by Schantz and co-workers. Extracts of the hepatopancreas of Alaskan butter clams (*Saxidomus giganteus*) yielded a highly toxic amorphous substance,

(1) For reviews on saxitoxin and related natural products, see: (a) Schantz, E. J. *Pure Appl. Chem.* **1980**, *52*, 183. (b) Shimizu, Y. In *Progress in the Chemistry of Organic Natural Products*: Herz, W., Grisebach, H., Kirby, G. W., Eds.; Springer-Verlag: New York, 1984; p 235. (c) Shimizu, Y. In *Marine Natural Products*; Scheuer, P. J., Ed.; Academic Press: New York, 1978; Vol. I, p 1.

0002-7863/92/1514-7001$03.00/0